J|A|C|S
ARTICLES
Published on Web 08/05/2004

TEM Investigation of Formation Mechanism of Monocrystal-Thick *b*-Oriented Pure Silica Zeolite MFI Film

Shuang Li,[†] Zijian Li,[†] Krassimir N. Bozhilov,[‡] Zhongwei Chen,[†] and Yushan Yan*,[†]

Contribution from the Department of Chemical and Environmental Engineering and Central Facility for Advanced Microscopy and Microanalysis, University of California, Riverside, California 92521

Received April 14, 2004; E-mail: Yushan.Yan@ucr.edu

Abstract: The first direct transmission electron microscopic (TEM) observation has been carried out on the continuous monocrystal-thick *b*-oriented pure silica zeolite MFI films produced by in situ crystallization. The self-supporting film samples for TEM study were fabricated by dissolving the steel substrate with acid. This TEM study is free of those artifacts that are typically associated with TEM sample preparations, and allows us to investigate the "true" structure and texture of a very large area of the film and at the same time to focus at will on each individual zeolite crystal in the film. Abundant TEM information including crystallographic orientation relationships among crystals in the film (both out-of-plane and in-plane), grain boundaries, and each crystal grain was obtained. This TEM investigation provides direct unambiguous new evidence to support the homogeneous nucleation mechanism, by which the films form through homogeneous nucleation and crystal growth in the bulk to form equal-sized disk-shape crystals, followed by self-assembly of these crystals onto the substrate to produce a two-dimensional close-packed structure. The last stage of the film formation involves simultaneous space-limited growth and rotation of the individual crystals to realize the in-plane crystallographic control within the film.

Introduction

There has been growing interest in the preparation of zeolite films with controlled crystal orientation. Appropriate orientation of the nanometer-sized channels in the zeolite crystals can drastically affect the mass transport behavior within a zeolite film, and this is crucial for its applications as separation membranes, membrane reactors, and chemical sensors.[1] For instance, a dramatic performance improvement has been observed in the xylene isomer separation through *b*-oriented MFI zeolite films versus *a*- and *c*-oriented zeolite membranes.[2] Very recently, molecular sieving was demonstrated for monolayer-thick *b*-oriented pure silica zeolite MFI film on stainless steel electrode.[3] A *b*-oriented MFI film was also successfully utilized as an inorganic host to accomplish molecular alignment for nonlinear optics applications.[4,5] Several approaches have been developed for preparing oriented zeolite films and layers.[6−15] Among them, templated in situ growth[6,7] and assembly of preformed zeolite crystals by organic linkages[8] could produce oriented zeolite crystals, but the obtained layers were not continuous. Also, in the latter case, the adhesion between the zeolite film and the substrate was very weak. Seeded growth method[2,11,12] could generate continuous oriented zeolite LTA and *b*,*c*-oriented MFI. However, the success is limited by the available shapes/sizes, deposition methods of the seed particles, and techniques to adjust the relative crystal plane growth rates. In an effort to extend the seeded growth process to other molecular sieve types and orientations, the heteroepitaxial growth method was developed.[13,15] However, this method only produced very small and isolated zeolite crystals that have a structure matching that of the substrate. In our previous work, a simple direct in situ crystallization method was developed to synthesize continuous *b*-oriented thin pure silica zeolite (PSZ) MFI monolayer films.[16,17] This method does not require any pretreatments of substrates. This film has a monolayer structure, which ensures a very thin film thickness (∼0.4 μm) and

[†] Department of Chemical and Environmental Engineering.
[‡] Central Facility for Advanced Microscopy and Microanalysis.

(1) Caro, J.; Noack, M.; Kolsch, P.; Schafer, R. *Microporous Mesoporous Mater.* **2000**, *38*, 3−24.
(2) Lai, Z. P.; Bonilla, G.; Diaz, I.; Nery, J. G.; Sujaoti, K.; Amat, M. A.; Kokkoli, E.; Terasaki, O.; Thompson, R. W.; Tsapatsis, M.; Vlachos, D. G. *Science* **2003**, *300*, 456−460.
(3) Li, S.; Wang, X.; Beving, D.; Chen, Z.; Yan, Y. *J. Am. Chem. Soc.* **2004**, *126*, 4122−4123.
(4) Davis, M. E. *Nature* **2002**, *417*, 813−821.
(5) Kim, H. S.; Lee, S. M.; Ha, K.; Jung, C.; Lee, Y. J.; Chun, Y. S.; Kim, D.; Rhee, B. K.; Yoon, K. B. *J. Am. Chem. Soc.* **2004**, *126*, 673−682.
(6) Feng, S.; Bein, T. *Science* **1994**, *265*, 1839−1841.
(7) Feng, S.; Bein, T. *Nature* **1994**, *368*, 834−836.
(8) Ha, K.; Lee, Y. J.; Chun, Y. S.; Park, Y. S.; Lee, G. S.; Yoon, K. B. *Adv. Mater.* **2001**, *13*, 594−596.
(9) Scandella, L.; Binder, G.; Gobrecht, J.; Jansen, J. C. *Adv. Mater.* **1996**, *8*, 137−139.
(10) Caro, J.; Finger, G.; Kornatowski, J.; Richtermendau, J.; Werner, L.; Zibrowius, B. *Adv. Mater.* **1992**, *4*, 273−276.
(11) Boudreau, L. C.; Tsapatsis, M. *Chem. Mater.* **1997**, *9*, 1705−1709.
(12) Gouzinis, A.; Tsapatsis, M. *Chem. Mater.* **1998**, *10*, 2497−2504.
(13) Okubo, T.; Wakihara, T.; Plevert, J.; Nair, S.; Tsapatsis, M.; Ogawa, Y.; Komiyama, H.; Yoshimura, M.; Davis, M. *Angew. Chem., Int. Ed.* **2001**, *40*, 1069−1071.
(14) Jeong, H. K.; Krohn, J.; Sujaoti, K.; Tsapatsis, M. *J. Am. Chem. Soc.* **2002**, *124*, 12966−12968.
(15) Wakihara, T.; Yamakita, S.; Iezumi, K.; Okubo, T. *J. Am. Chem. Soc.* **2003**, *125*, 12388−12389.
(16) Wang, Z. B.; Yan, Y. S. *Microporous Mesoporous Mater.* **2001**, *48*, 229−238.
(17) Wang, Z. B.; Yan, Y. S. *Chem. Mater.* **2001**, *13*, 1101−1107.

10.1021/ja0478429 CCC: $27.50

eliminates grain boundaries that will be crossed by permeating molecules because in the monolayer film only grain boundaries that are perpendicular to the support surface exist. Moreover, due to the preferred *b*-orientation and the monolayer nature of the film, the straight channels in MFI are perpendicular to the substrate surface and through the whole film thickness. All these features are favorable for molecular diffusion and ensure high fluxes. In addition, these films have excellent adhesion on various substrates such as silicon, aluminum, steel, and silica, making this in situ method the simplest and most versatile method for fabricating *b*-oriented monolayer MFI films.

To further optimize the synthesis conditions and to potentially generalize this control strategy to other orientations and other types of zeolites, a fundamental understanding of the film formation mechanism is of great significance. Although extensive efforts have been made toward this end, the true film formation mechanism remains elusive. A heterogeneous nucleation (HTN) model was proposed previously[18−20] and was widely cited. With this model, a gel layer is first formed on the surface of the substrate and then nucleation and crystal growth occur at the solid and solution interface. This model can explain well the fact that *b*-oriented crystals are formed on both horizontally and vertically placed substrates, but it has difficulty in explaining why *a*-oriented crystals appear in the film sometimes and why second layer is present under certain conditions. It is also difficult for this model to explain the excellent adhesion that has been observed between the zeolite film and the substrate.[16] We have proposed a homogeneous nucleation (HMN) model previously.[16,17] With this model, nucleation occurs homogeneously in the bulk solution and the nuclei grow into small disk-shape crystals with {010} as the largest flat surfaces. Since under the particular pH the interaction between the crystals and the surface is favorable,[21] it is energetically preferred for these crystals to settle onto the substrate with *b*-oriented positions. This model can explain well all of our previous experimental observations.[16]

Although logical and consistent, all of the previous evidence in support of the HMN model was circumstantial. In the present study, we provide the first direct, unambiguous transmission electron microscopic (TEM) evidence to support the HMN mechanism. We have taken advantage of the fact that pure silica zeolite and high silica zeolite films are extremely corrosion resistant.[22,23] The self-supporting MFI films were thus simply prepared by growing *b*-oriented MFI films on very thin stainless steel foil substrates and subsequently removing the substrate by acid etching. Thanks to the remarkable mechanical integrity and the small thickness of the films, the self-supporting film can be studied in the TEM directly. This approach gives us an unique opportunity to investigate the "true" three-dimensional texture and structure of the film without an artificially created interference that can be introduced by the most commonly used TEM specimen preparation methods such as cutting the zeolite crystals into thin slices with an ultramicrotome or ion milling.[24] The area of the film and the number of crystals that can be analyzed within one sample and the extent and accuracy of information obtained about the film texture and orientation are unprecedented.

Experimental Section

The *b*-oriented pure silica zeolite (PSZ) MFI films were prepared as follows. The synthesis mixture was prepared by slowly adding tetraethyl orthosilicate (TEOS, Aldrich) to a solution of tetrapropylammonium hydroxide (TPAOH, Sachem) in water under stirring, and the solution was aged for 4 h under stirring at room temperature. The final molar composition of the synthesis solution was 0.32 TPAOH:1 TEOS:165 H_2O. Then 20 g of the synthesis solution was loaded to a 45 mL Teflon-lined Parr autoclave where the stainless steel foil was placed at the bottom vertically. Crystallization was carried out at 165 °C for 2−3 h. The samples were recovered and thoroughly washed with deionized water and blow-dried in N_2 stream. Stainless steel foil substrate (0.002 in. thickness, McMaster-Carr) was thoroughly washed in deionized water under ultrasonication before using.

The morphology of the MFI films was studied by scanning electron microscopy (SEM; FEI-Philips XL30-FEG instrument at 20 kV). X-ray diffraction (XRD) patterns of zeolite films were obtained on a Siemens D-500 diffractometer using Cu Kα radiation. All TEM specimens were prepared by dissolving the stainless steel substrate in 10% HCl solution at room temperature. The obtained transparent green solution containing the zeolite self-supporting film was rinsed several times until it became colorless; after that it was ultrasonicated for 10 min to break the film into smaller pieces. A drop of the resulting suspension was deposited onto Cu grids coated with a thin (5 nm thickness) holey carbon support film. For high-resolution TEM (HRTEM) imaging the zeolite films were polished for about 10 min with 0.05 μm Al_2O_3 suspension using a Buehler polisher to remove the second layer crystals and to reduce the thickness of the film before dissolving the stainless steel substrate. TEM was performed with a FEI-Philips CM300 microscope operating at 300 kV accelerating voltage, equipped with a LaB_6 electron gun and a twin objective lens. The HRTEM images were obtained with a 50 μm diameter condenser aperture, effective objective aperture radius of 0.49 nm^{-1}, spherical aberration (C_s) of 2.00 mm, at defocus values of +120 to −160 nm and beam convergence angle of 0.8 mrad. Images were recorded digitally using a Gatan 794 MultiScan CCD camera and Gatan Microscopy Suite 1.2 software. HRTEM image interpretation is based on comparison with published data and image simulation, which was performed using the multislice approach and MacTempas software.

Results and Discussion

The zeolite crystals form a continuous film on stainless steel foil (Figure 1a), and the film is about 0.3−0.4 μm thick (Figure 1b). From SEM images and the crystal shape, it appears that the film has a monolayer structure where zeolite single crystals are close-packed and oriented with their {010} planes parallel to the substrate. This is illustrated in Figure 1c. Only (0*k*0) lines are present in the XRD pattern of the zeolite film, confirming that the crystals are *b*-oriented (Supporting Information Figure S-1).

A second layer of zeolite crystals is also observed on many occasions (Figure 1a,b). The second layer is not continuous and consists of isolated crystals, which are oriented with either {010} or {100} parallel to the substrate. For lattice imaging (HRTEM), the films were slightly polished before acid etching of the substrate to remove the loose second layer crystals and to reduce

(18) den Exter, M. J.; van Bekkum, H.; Rijn, C. J. M.; Kapteijn, F.; Moulijn, J. A.; Schellevis, H.; Beenakker, C. I. N. *Zeolites* **1997**, *19*, 13−20.
(19) Koegler, J. H.; van Bekkum, H.; Jansen, J. C. *Zeolites* **1997**, *19*, 262−269.
(20) Jansen, J. C.; Vanrosmalen, G. M. *J. Cryst. Growth* **1993**, *128*, 1150−1156.
(21) Lai, R.; Yan, Y. S.; Gavalas, G. R. *Microporous Mesoporous Mater.* **2000**, *37*, 9−19.
(22) Cheng, X. L.; Wang, Z. B.; Yan, Y. S. *Electrochem. Solid State* **2001**, *4*, B23−B26.
(23) Mitra, A.; Wang, Z. B.; Cao, T. G.; Wang, H. T.; Huang, L. M.; Yan, Y. S. *J. Electrochem. Soc.* **2002**, *149*, B472−B478.
(24) Sasaki, Y.; Shimizu, W.; Ando, Y.; Saka, H. *Microporous Mesoporous Mater.* **2000**, *40*, 63−71.

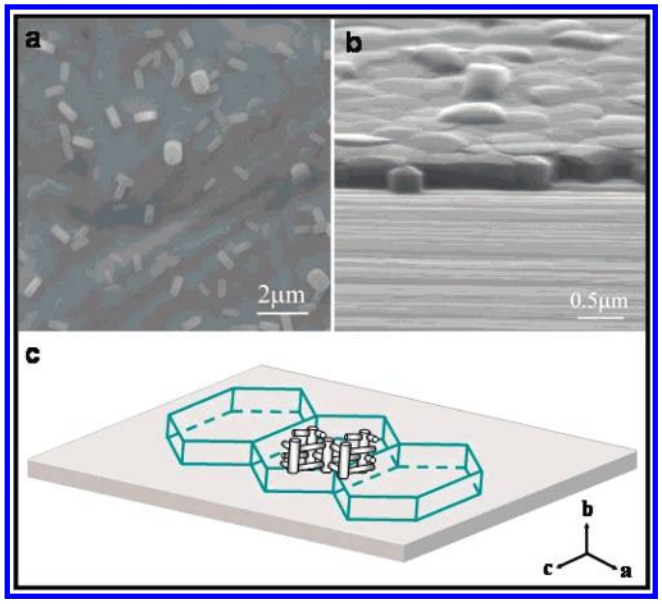

Figure 1. Scanning electron micrographs (SEM) of (a) top view of in situ *b*-oriented pure silica zeolite (PSZ) MFI films on stainless steel, (b) cross-sectional view of (a), and (c) schematic of the pore structure of *b*-oriented PSZ MFI zeolite film.

their thickness. After polishing, a smooth and featureless surface was obtained. No cracking and peeling off of the film during polishing was observed, which indicates excellent mechanical strength and adhesion of the film. Since the focus of this study is the film formation mechanism, the discussion hereafter will focus on the first layer crystals.

After dissolving of the stainless steel substrate in acid solution, the self-supporting zeolite films have very good mechanical integrity. They are transparent and the copper TEM grid underneath can be clearly seen from low magnification SEM images (Figure 2a). In the low magnification bright-field (BF) TEM images (Figure 2b), both first layer and second layer crystals can be observed with clear grain boundaries that have been very difficult to distinguish in a SEM image with comparable magnification (Figure 1a). Moreover, high magnification TEM images show strikingly regular honeycomb close packing of hexagon-shape zeolite crystals, and no obvious surface defects or grain boundary defects were observed at this magnification (Figure 2b−d). The contrast difference between individual crystals is due to diffraction contrast caused by the slight inclination of the {010} planes of the individual crystals with respect to the film surface, causing some crystals to be oriented closer to strong diffracting (Bragg) orientation compared to their neighbors.

Applying selected area electron diffraction (SAED), we have examined in great detail more than 40 individual crystals to determine the crystallographic orientation relationships between individual crystals. It was found that the *b* axes of the crystals are slightly tilted from the normal to the plane of the film. The tilt is in random directions and the *b* axes of adjacent zeolite crystals are not parallel but form an angle of about 2°−8° with respect to each other (Figure 2d, inset). The lack of deformations, cracks, and/or pronounced dislocation density at the crystal interfaces suggests that this tilt is not an artifact from the processing (e.g., acid etching and rinsing) of the film after the synthesis, but rather it represents the original structure of the film.

The orientation of the zeolite crystals within the plane was also determined (Figure 2d), which demonstrates that the crystals are rotated around their *b* axes with respect to each other. The grain boundary orientation between adjacent crystals is not random and exhibits strongly pronounced crystallographic control. In general, each crystal has a hexagon shape and is confined by six crystal interfaces. The orientation of the interfaces is controlled by prominent crystallographic directions in the crystals, and the grain boundaries are subparallel or make very small angles with the {100} and {101} faces for about 80% of the measured crystals (e.g., Figure 2d, nos. 1−6, 8). It is noted that these crystals have the same shape and forms as

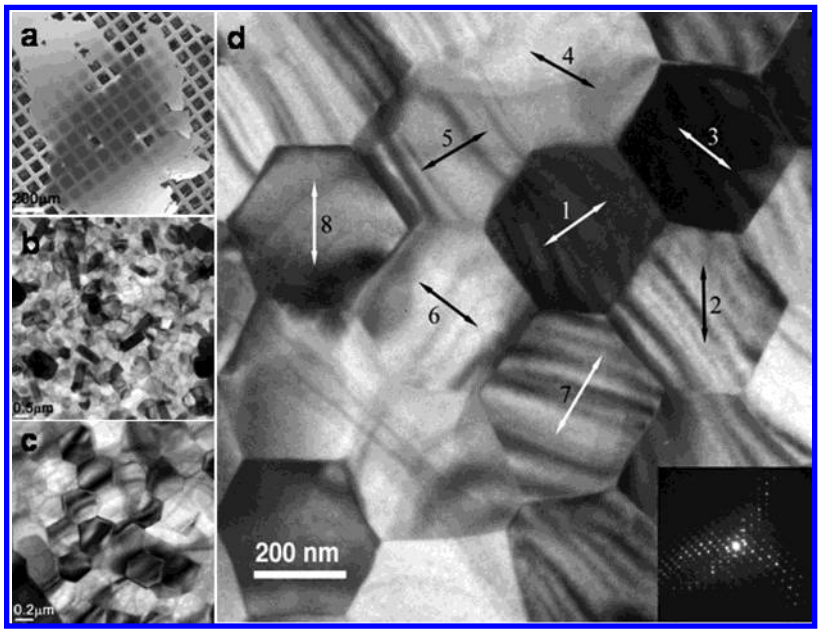

Figure 2. SEM and TEM micrographs of the zeolite film after dissolution of the stainless steel substrate: (a) low magnification SEM image showing the self-standing *b*-oriented MFI zeolite film on a TEM grid; (b) low magnification TEM image showing the MFI zeolite monolayer consisting of uniform close-packed hexagon-shape zeolite crystals; (c, d) high magnification TEM images of the *b*-oriented film. In (d) the orientation of the ⟨100⟩ direction is shown by arrows for eight of the crystals. Inset in (d) shows the SEAD pattern down {010} taken at the interface of two crystals.

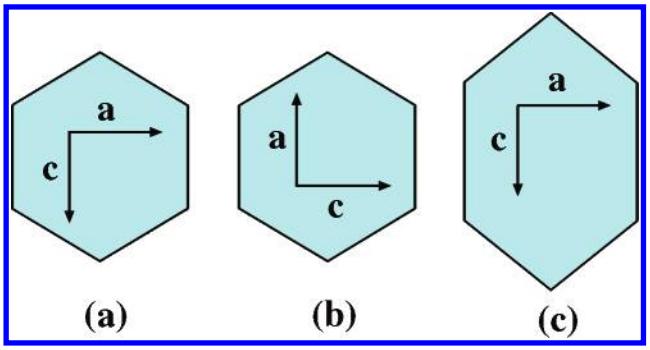

Figure 3. Schematic drawing of MFI crystal shapes. (a) Hexagon-shape crystal (short) in our synthesized film (equilibrium faces {100} and {101} are well developed, Figure 2d, nos. 1−6, no. 8). (b) Hexagon-shape crystals as shown in our synthesized film (nonequilibrium faces such as {001} are developed, Figure 2d, no. 7). (c) Equilibrium habit of crystal growing in a free environment. Growth along the *c* axis is fastest and correspondingly well-developed {100} faces are formed.

the crystals that have been grown in a free environment (Figure 3). However, their dimension along ⟨001⟩ is shorter. For the rest of the crystals (∼20%), the interfaces are parallel or closely parallel to the {001} and {101} faces (e.g., Figure 2d, no. 7). Note that the {001} faces do not usually develop under the synthesis conditions in a free equilibrium environment (Figure 3). The interfaces of adjacent crystals form triple junctions, and the angle between them is close to but usually different from 120°. The majority of the angles between the interfaces vary from about 110° to 128°, and for some crystals the distortion of the shape from a regular hexagon is more pronounced and interface angles around 100°−135° can be observed. Another important feature of the film is the uniform size of the individual crystals. Their diameters are around 300−350 nm, and no significant variation is observed beyond these dimensions.

HRTEM imaging was applied to reveal the atomic structure of the zeolite crystals and to characterize more closely the structure of the interfaces (Figure 4). The individual crystals have perfect internal structure, and no defects were observed by lattice imaging. To facilitate interpretation, HRTEM images were simulated for the utilized experimental conditions and they closely match the lattice images obtained experimentally (Figure 4a, inset). At Scherzer defocus the white spots in the lattice images taken down {010} correspond to the position of the open channels parallel to the *b* axis. This allows direct interpretation of the lattice images in terms of the crystal structure at the unit cell level. As visualized by HRTEM (Figure 4), the crystal interfaces for most of the crystals are not perfectly parallel to low index atomic planes and form small angles (2°−8°) with the {100}, {101}, or {001} planes. The structure of the interface has stepwise character. Usually the steps are parallel to low index crystallographic directions such as ⟨100⟩, ⟨101⟩, and ⟨001⟩. The interfaces are coherent and no distortion of the atomic planes has been observed. From the HRTEM images, it was difficult to determine whether the channels are continuous at the grain boundaries between crystals.

The shape, size, packing, and orientation of the zeolite crystals in the film observed by TEM can shed light on the film formation mechanism and allow a closer examination of possible models. According to the HTN model[18−20] a silica gel layer is formed on the surface of silicon wafer substrate. Nucleation occurs only at the gel−solution interface, where both the structure-directing agent (TPA) and the silica source are present in abundance. Crystal growth proceeds into the gel phase by consuming the gel layer until the crystals bond with the substrate and finally align with their {010} faces parallel to the substrate. This model can explain well the fact that {010} oriented crystals are formed on both horizontally and vertically placed substrates, but it is difficult to use this model to explain why {100} oriented crystals appear in the film sometimes and why a second layer is present under certain conditions. More important, the HTN model has profound difficulty in explaining the uniform size and patterned arrangement of the zeolite crystals observed in this study. We did not observe significant deviation in the crystal size for a significant number of samples from multiple sets of experiments. To achieve the uniform crystal size distribution, according to the HTN model, nucleation must be absolutely homogeneous so that all nuclei are equal distance from each other. Only if this condition was satisfied could a uniform crystal size distribution, hexagonal close packing, and the observed honeycomb structure possibly be obtained. The chance of such homogeneous nucleation in the gel layer is very small due to lower diffusion rates in the gel. Another possible explanation of the observed structures based on the HTN model could be that, although nucleation is not homogeneous, later development

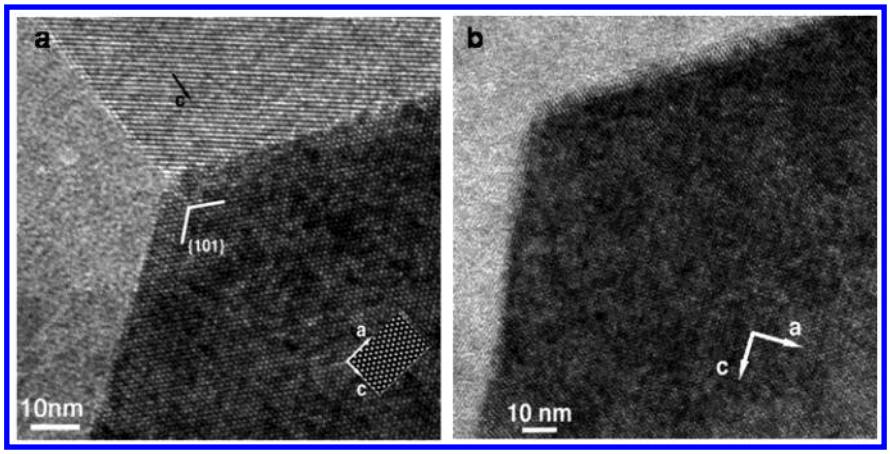

Figure 4. HRTEM images taken down the *b* axis of MFI crystals in which the crystal lattice is visualized. The interfaces of the crystals are inclined slightly with respect to the {100} and {101} planes. The interfaces of the crystal in (a) are subparallel to {101}, whereas in (b) the interfaces are subparallel to {100} and {101}. The structure of the interface has stepwise character. Usually the steps are parallel to low index crystallographic directions. The interfaces are coherent and no distortion of the atomic planes has been observed. As an inset in (a) is shown an 8 × 8 unit cell segment of a simulated HRTEM image down {010}. The white spots can be attributed to the positions of the open channels parallel to *b*.

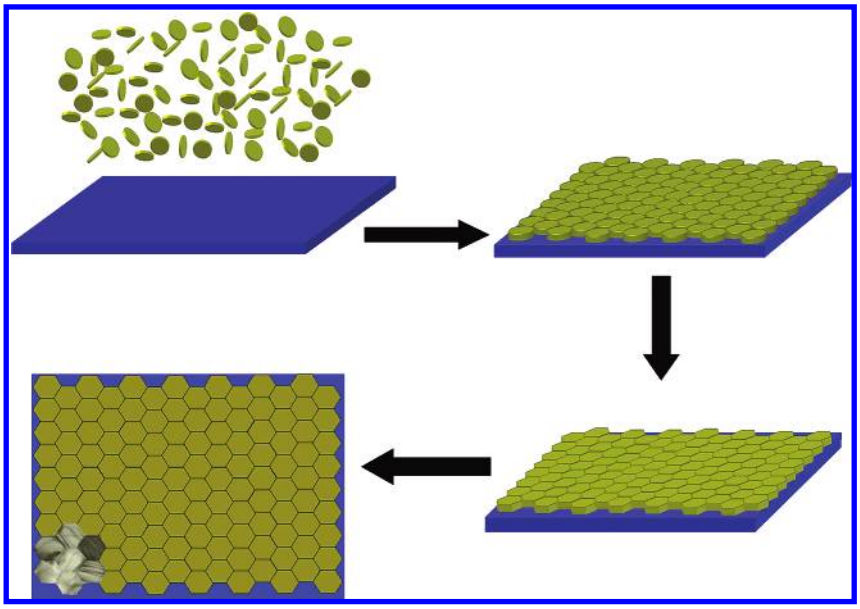

Figure 5. Schematic diagram of the proposed formation mechanism for *b*-oriented zeolite MFI thin film. (a) Nucleation and crystal growth of colloidal disk-shape submicron crystals in the bulk. (b) Self-assembly of colloidal disk-shape crystals onto the substrate. (c) Formation of a continuous zeolite film consisting of close-packed hexagon-shape crystals. (d) Top view of (c) with a portion of the TEM image inserted at the lower left corner of the drawing showing the excellent match between the TEM image and the drawing.

of Ostwald ripening of the crystal can lead to dissolution of the very small crystals and growth of almost equally sized crystals if the surface of the substrate is absolutely homogeneous and if the small crystals are randomly and uniformly distributed. Even this highly unlikely assumption fails to explain the high degree of in-plane crystallographic control of the zeolite crystals that has been commonly observed in our experiments. The attainment of the observed structure following the HTN model of crystallization would require that during the Ostwald ripening process the crystals are mobile and they can move, rotate, and arrange themselves according to the rules of two-dimensional hexagonal close packing. Such a requirement for mobility of the crystals is contradictory to the actual HTN mechanism of growth, where the attachment to a gel layer is a necessary prerequisite. The presence of the gel layer will also inhibit the mobility of components and impair the capability for uniform nucleation and growth.

An alternative HMN mechanism was proposed[16] for the formation of the in situ *b*-oriented zeolite film (Figure 5). According to this mechanism, in the initial stage, colloidal submicron crystals (<0.5 μm) form. Then, these submicron zeolite crystals undergo a self-assembly deposition process on the substrate surface to form a nearly continuous layer due to favorable electrostatic and van der Waals interactions.[21,25] Since these submicron MFI crystals are shaped like disks (the {010} plane has the largest surface area), the most stable configuration for them to settle onto the surface is to lie on their flat surface, that is {010} parallel to the substrate. The close packing and *b*-orientation of the disk-shape crystals on the substrate is evident in the early stage of film formation (Figure 6). The in-plane orientations of the crystals are likely to be random at this time. Then the submicron crystals inside the film continue to grow (only to fill the gap between the disk-shape crystals) and begin to merge due to limited space between the crystals. At this time,

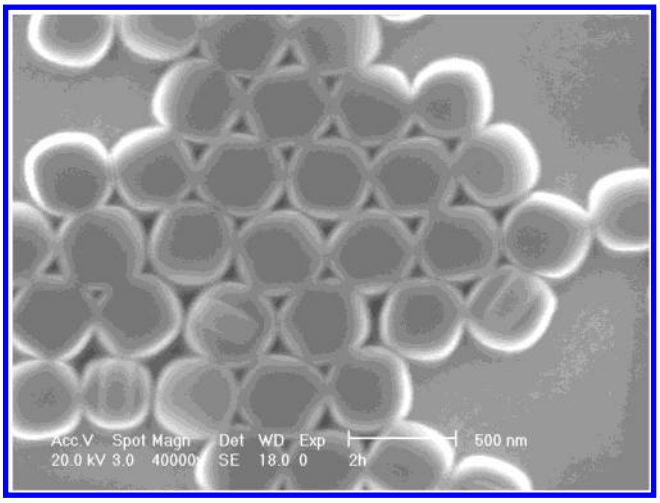

Figure 6. SEM image of zeolite crystals at the early stage of film formation (synthesis time 2 h). The film is not continuous, which is due probably to the loss of some of the zeolite crystals during the sample recovery process (e.g., washing and rinsing), since during that stage the crystals are not yet firmly attached to the substrate.

the precursor crystals have a certain mobility, so they can rotate and rearrange in small angles to find a crystallographically favorable position before their final merger with their neighboring crystals. Eventually uniform hexagon-shape crystals develop and form the close-packed honeycomb pattern. Note that to achieve the in-plane crystallographic control observed, a maximum 30° rotation is needed for any particular crystal. It is likely, however, that the neighboring crystals act in coordination during the rotation, and thus each crystal only needs to rotate an angle much smaller than 30° to avoid paying a high energetic penalty. The fact that ~20% of the crystals have developed nonequilibrium faces (Figure 2d, no. 7) can be a result that these crystals were trapped by their neighbors and were not allowed to realize the desired rotation and were forced to grow in the direction of the available open space. Another confirmation of the proposed mechanism is the slight inclination of the *b* axes

(25) Myatt, G. J.; Budd, P. M.; Price, C.; Carr, S. W. *J. Mater. Chem.* **1992**, *2*, 1103−1104.

of almost all crystals from the normal to the substrate. The crystal nuclei which deposited on the substrate possessed a disk-shape habit and their {010} faces were not perfectly flat; rather, they show a curved character (Figures 1b and 6). This curved surface caused the crystals to settle down with a slight tilt with respect to the substrate. The consequent growth preserved this initial tilt, which is proportional to the degree of curvature of the {010] faces of the original disk-shape nuclei.

The fact that the crystals that have self-assembled onto the substrate in the early stage of film formation (in Figure 6) are roughly equal in size to the hexagons in the final zeolite film (Figure 2d) is consistent with this space-limited growth mechanism. The effect of space limitation on crystal growth in the first layer was also clearly reflected by the difference in shape and dimension between the crystals from the first layer (Figure 2d) and those from the second layer (Figure 1a). While the second layer crystals are elongated prisms, the crystals in the film are isometric hexagons (Figure 2d).

In summary, we have prepared a very robust self-supporting MFI zeolite film by growing the {010} *b*-oriented film on very thin stainless steel foil substrate and subsequently removing the substrate by acid etching. The self-standing films show remarkable mechanical integrity and thin thickness, and thus can be studied directly by TEM. TEM results provided direct and convincing evidence for our previously proposed homogeneous nucleation mechanism. Also, this TEM study establishes unambiguously that the MFI film is a monocrystal thick, and provides detailed information about the overall film orientation, the crystallographic orientation relationships among crystals, the structure and orientation of the interfaces, and the individual crystal growth steps during the film formation.

Acknowledgment. We thank SERDP/DoD, TSE/EPA, and NSF (CTS-0404376) for financial support.

Supporting Information Available: XRD pattern of *b*-oriented MFI zeolite film and MFI powder. This material is available free of charge via the Internet at http://pubs.acs.org.

JA0478429